Video Article

Generating Controlled, Dynamic Chemical Landscapes to Study Microbial Behavior

Francesco Carrara[1], Douglas R. Brumley[2], Andrew M. Hein[3], Yutaka Yawata[4,5], M. Mehdi Salek[1], Kang Soo Lee[1], Elzbieta Sliwerska[1], Simon A. Levin[6], Roman Stocker[1]

[1]Institute of Environmental Engineering, Department of Civil, Environmental and Geomatic Engineering

[2]School of Mathematics and Statistics, University of Melbourne

[3]Institute of Marine Sciences, University of California, Santa Cruz

[4]Faculty of Life and Environmental Sciences, University of Tsukuba

[5]Microbiology Research Center for Sustainability, University of Tsukuba

[6]Department of Ecology and Evolutionary Biology, Princeton University

Correspondence to: Francesco Carrara at carraraf@ethz.ch, Roman Stocker at romanstocker@ethz.ch

URL: https://www.jove.com/video/60589
DOI: doi:10.3791/60589

Keywords: Bioengineering, Issue 155, caged compounds, chemical pulses, chemotaxis, microbial ecology, microfluidics, motility, photolysis, polycarbonate membrane

Date Published: 1/31/2020

Citation: Carrara, F., Brumley, D.R., Hein, A.M., Yawata, Y., Salek, M.M., Lee, K.S., Sliwerska, E., Levin, S.A., Stocker, R. Generating Controlled, Dynamic Chemical Landscapes to Study Microbial Behavior. *J. Vis. Exp.* (155), e60589, doi:10.3791/60589 (2020).

Abstract

We demonstrate a method for the generation of controlled, dynamic chemical pulses—where localized chemoattractant becomes suddenly available at the microscale—to create micro-environments for microbial chemotaxis experiments. To create chemical pulses, we developed a system to introduce amino acid sources near-instantaneously by photolysis of caged amino acids within a polydimethylsiloxane (PDMS) microfluidic chamber containing a bacterial suspension. We applied this method to the chemotactic bacterium, *Vibrio ordalii*, which can actively climb these dynamic chemical gradients while being tracked by video microscopy. Amino acids, rendered biologically inert ('caged') by chemical modification with a photoremovable protecting group, are uniformly present in the suspension but not available for consumption until their sudden release, which occurs at user-defined points in time and space by means of a near-UV-A focused LED beam. The number of molecules released in the pulse can be determined by a calibration relationship between exposure time and uncaging fraction, where the absorption spectrum after photolysis is characterized by using UV-Vis spectroscopy. A nanoporous polycarbonate (PCTE) membrane can be integrated into the microfluidic device to allow the continuous removal by flow of the uncaged compounds and the spent media. A strong, irreversible bond between the PCTE membrane and the PDMS microfluidic structure is achieved by coating the membrane with a solution of 3-aminopropyltriethoxysilane (APTES) followed by plasma activation of the surfaces to be bonded. A computer-controlled system can generate user-defined sequences of pulses at different locations and with different intensities, so as to create resource landscapes with prescribed spatial and temporal variability. In each chemical landscape, the dynamics of bacterial movement at the individual scale and their accumulation at the population level can be obtained, thereby allowing the quantification of chemotactic performance and its effects on bacterial aggregations in ecologically relevant environments.

Video Link

The video component of this article can be found at https://www.jove.com/video/60589/

Introduction

Microbes rely on chemotaxis, the process of detecting chemical gradients and modifying motility in response[1], to navigate chemical landscapes, approach nutrient sources and hosts, and escape noxious substances. These microscale processes determine the macroscale kinetics of interactions between microbes and their environment[2,3]. Recent advances in microfluidics and microfabrication technologies, including soft lithography[4], have revolutionized our ability to create controlled microenvironments in which to study the interactions of microbes. For example, past experiments have studied bacterial chemotaxis by generating highly controlled, stable gradients of intermediate to high nutrient concentrations[5,6]. However, in natural environments, microscale chemical gradients can be short-lived—dissipated by molecular diffusion—and background conditions are often highly dilute[7]. To directly measure the chemotactic response of microbial populations first exposed to unsteady chemical environments, we devised and here describe methods to combine microfluidic technology with photolysis, thereby mimicking gradients that wild bacteria encounter in nature.

Uncaging technology employs light sensitive probes that functionally encapsulate biomolecules in an inactive form. Irradiation releases the caged molecule, allowing the targeted perturbation of a biological process[8]. Due to the rapid and precise control of cellular chemistry that the uncaging affords[9], photolysis of caged compounds has traditionally been employed by biologists, physiologists and neuroscientists to study the activation of genes[10], ion channels[11], and neurons[12]. More recently, scientists have leveraged the significant advantages of photolysis to study

chemotaxis[13], to determine the flagella switching dynamics of individual bacterial cells exposed to a stepwise chemoattractant stimulus[14,15], and to investigate motility patterns of single sperm cells in three-dimensional (3D) gradients[16].

In our approach, we implement photolysis of caged amino acids within microfluidic devices to study the behavioral response of a bacterial population to controlled chemical pulses, which become near-instantaneously available through photorelease. The use of a low-magnification (4x) objective (NA = 0.13, depth of focus approximately 40 µm) allows both the observation of the population-level aggregative response of thousands of bacteria over a large field of view (3.2 mm x 3.2 mm), and the measurement of motion at the single-cell level. We present two applications of this method: 1) the release of a single chemical pulse to study bacterial accumulation−dissipation dynamics starting from uniform conditions, and 2*i*) the release of multiple pulses to characterize the bacterial accumulation dynamics under time-varying, spatially heterogeneous chemoattractant conditions. This method has been tested on the marine bacteria *Vibrio ordalii* performing chemotaxis toward the amino acid glutamate[17], but the method is broadly applicable to different combinations of species and chemoattractants, as well as to biological processes beyond chemotaxis (e.g., nutrient uptake, antibiotic exposure, quorum sensing). This approach promises to help elucidate the ecology and behavior of microorganisms in realistic environments and to uncover the hidden trade-offs that individual bacteria face when navigating ephemeral dynamic gradients.

Protocol

1. Fabrication of the Microfluidic Device for the Single Chemical-pulse Experiment

1. Design the channel using computer-aided design (CAD) software and print it onto a transparency film to create the photo mask (**Figure 1A**).
2. Fabricate the master by soft lithography (under clean-room conditions).
    1. Clean a silicon wafer (4 inches) in quick succession with acetone, methanol and isopropanol, then dry using nitrogen. Bake the wafer in the oven at 130 °C for 5 min.
    2. Place the wafer at the center of a spin-coater and pour SU-8 photoresist onto the wafer. Ramp the speed of the spin-coater up to 500 rpm over 5 s, and keep at 500 rpm for 10 s. Ramp up to the final speed over 10 s and maintain at this speed for 30 s.
    NOTE: The exact value of the final speed depends on the targeted coating thickness and the SU-8 used.
    3. After the spin-coating process, bake the wafer at 65 °C and then at 95 °C. Let the wafer cool at room temperature (RT) for at least 5 min.
    NOTE: The baking time depends on the targeted thickness and type of photoresist used. As a general rule, for every 100 µm layer the wafer should be baked for 5 min at 65 °C and 45 min at 95 °C.
    4. Place the photo mask onto the wafer to ensure that just the region of interest is exposed and polymerized. Expose to UV light for the time recommended in the SU-8 manual.
    NOTE: Here, with exposure energy of 200 mJ cm^{-2} at a wavelength of 350 nm, the wafer was exposed for 150 s.
    5. Bake the wafer at 65 °C and 95 °C for the time recommended in the SU-8 manual.
    NOTE: As a general rule, for every 100 µm layer the wafer should be baked for 5 min at 65 °C and 45 min at 95 °C.
    6. Immerse the wafer in a beaker filled with polymethyl methacrylate (PMMA) developer in order to obtain the master. Gently shake the beaker to ensure that the unpolymerized photoresist is washed out. Bake the master at 200 °C to further cross-link the SU-8 layer.
3. Prepare a polydimethylsiloxane (PDMS) mixture by combining the elastomer with its curing agent (**Table of Materials**) at a 10:1 ratio in a beaker (here, 40 mL). Mix vigorously until the liquid is homogeneous.
NOTE: The PDMS mixture will look opaque because bubbles are generated during the mixing process.
CAUTION: In order to prevent skin coming into contact with potentially hazardous chemicals or biological material, always wear a lab coat and disposable plastic gloves throughout the protocol and follow any specific safety protocols according to the Material Safety Data Sheet (MSDS).
4. Degas the PDMS mixture in a vacuum chamber for 45 min at RT. To expedite the process, periodically release the vacuum in order to burst the bubbles that form at the interface.
NOTE: The degassing process must be performed within 1 h to prevent the PDMS mixture from beginning to cure.
5. Remove dust from the surface of the master with a pressurized cleaner, then pour the degassed PDMS mixture onto the master and bake in an oven at 80 °C for 2 h.
NOTE: Alternatively, baking overnight (or for at least 12 h) at 60 °C would achieve the same hardened PDMS.
6. Cut the PDMS with a blade around the microstructures (at a distance of approximately 5 mm) and then carefully peel the PDMS from the master.
7. Punch holes to serve as inlet and outlet of the microchannel (here, one inlet and one outlet, see **Figure 1A**). Ensure that nothing touches the bottom face of the PDMS where the features are located.
NOTE: The protocol can be paused here. The microchannel should be sealed with adhesive tape to prevent accumulation of dust and other particles during storage.
8. Bond the PDMS microchannel to a glass slide.
    1. Thoroughly clean a glass slide with soap, isopropanol and deionized water. Let the glass slide dry or use compressed air to speed up the process.
    2. Remove dust particles by dabbing with adhesive tape. Bond the PDMS microchannel on the clean glass slide, immediately after treating both surfaces with plasma (by using either a corona system or a plasma oxygen chamber) for 2 min.
    3. Place the microfluidic device to heat on a hot plate at 80 °C for at least 1 h to strengthen the chemical bond with the glass.

2. Fabrication of the 3D-printed Millifluidic Device for the Experiment with Multiple Pulses

1. Design the 3D shape using 3D-design software and print the master for the PDMS mold with a high-resolution 3D printer (**Figure 1B**).
NOTE: See **Table of Materials** for the 3D printer and mold material used to create the master.

2. Repeat steps 1.3−1.4, then clean the surface of the master by dabbing with adhesive tape. Put the master on a scale, then, while avoiding the central region of the master that will be occupied by the membrane, pour on the exact quantity of uncured PDMS mixture (here, 23.4 g) in order to obtain the desired height of PDMS by matching the height of the master (here, 0.5 mm). Remove any remaining bubbles with the help of compressed air.
3. Place the PDMS cast on the master in an oven at 45 °C to bake for at least 12 h.
4. Bond the 3D PDMS mold to a Petri dish.
    1. Gently peel off the hardened PDMS layer and punch inlet and outlet holes for the injection of the bacterial suspension (**Figure 1C**).
    2. Activate both the surface of a Petri dish (90 mm x 15 mm) and the PDMS mold with oxygen plasma for 2 min. Bond the PDMS mold on the Petri dish. Gently press the mold to the Petri dish, but do not press where the features are located as this can collapse the interrogation chamber.
    3. Place the Petri dish bonded to the PDMS 3D mold in an oven at 45 °C for at least 12 h to strengthen the chemical bond.
    NOTE: The protocol can be paused here.

5. Membrane surface functionalization[18]
    1. Activate the nanoporous polycarbonate (PCTE) membrane in an oxygen plasma chamber for 1 min at RT.
    CAUTION: Avoid using a corona system for the plasma activation because it will damage the membrane.
    2. Under a chemical hood, dilute a commercial solution of 3-aminopropyltriethoxysilane (APTES) in deionized water to 1% by volume (here, 40 mL), by using a polypropylene tube.
    CAUTION: The APTES solution is acutely toxic (MSDS health hazard score 3) and should be handled with extreme care exclusively under a chemical hood with gloves. Change gloves immediately after handling APTES solution. APTES fumes are destructive to the mucous membranes and the upper respiratory tract. The target organs of APTES are nerves, liver, and kidney. If a fume hood is not available, a face shield and full-face respirator must be implemented.
    3. Transfer the diluted APTES solution in a Petri dish and immerse the activated membrane in the APTES solution for 20 min.
    4. Remove the membrane from the APTES solution with tweezers and place it on a cleanroom wipe to dry.

6. For the fabrication of the PDMS microfluidic channels that will lie on the membrane and allow washing of the bacterial arena, repeat steps 1.1−1.7.
7. Bond the PDMS washing channels to the functionalized membrane.
    1. Activate both the PDMS washing channel and the PCTE membrane with an oxygen plasma chamber for 2 min.
    NOTE: The membrane, which will be sandwiched between two PDMS layers, should be smaller than the PDMS washing channel.
    2. Immediately after the plasma treatment, bring the functionalized membrane and the PDMS washing channel into contact by gently pressing the PDMS washing channel onto the membrane.
    NOTE: Do not apply excessive pressure at this stage, because it might cause (irreversible) attachment of the membrane to the channel's roof, blocking the channel.

8. Sandwich the membrane between two PDMS layers (**Figure 1E**).
    1. Activate both the bonded laminate PDMS washing channel−PCTE membrane and the 3D PDMS mold previously bonded to the Petri dish with an oxygen plasma chamber for 2 min. Bring them into contact and press together.
    2. Place the Petri dish bonded to the sandwich structure in an oven at 45 °C for at least 12 h to strengthen the chemical bond.
    NOTE: The protocol can be paused here.

3. Cell Culture

1. Grow a population of *V. ordalii* (strain 12B09 or 12B09pGFP) overnight for 20 h in 2216 medium[19] on an orbital shaker (600 rpm) at 30 °C and harvest cells in late-exponential phase. For isolates harboring pGFP, add spectinomycin (50 µg mL^{-1}) to maintain the plasmid.
2. Centrifuge a 1 mL aliquot of cells at 2500 x *g* for 3 min, remove the supernatant and re-suspend the cells in 1 mL of filtered artificial seawater. Repeat this step.
3. Starve the population of *V. ordalii* on an orbital shaker (600 rpm) at 30 °C for 3 h.
4. Prepare a stock artificial seawater solution of 10 mM (here, 1 mL) of 4-methoxy-7-nitroindolinyl-caged-*L*-glutamate (MNI-caged-*L*-glutamate) and store at -20 °C.
NOTE: Protect the MNI-caged-*L*-glutamate solution from ambient light to prevent photolysis.
5. Dilute the cells 50x by re-suspending the starved cells in an artificial seawater solution of 1 mM MNI-caged-*L*-glutamate.
NOTE: This will ensure a final bacterial concentration lower than 5 x 10^7 mL^{-1} (the exact value depends on the initial concentration of cells in late exponential, which is typically ~10^9 mL^{-1}). Bacterial concentration was estimated using a spectrophotometer at optical density (OD) of 600 nm.

4. Calibration of the Uncaging Protocol

1. Place a droplet (20 µL) of an artificial seawater solution of MNI-caged-*L*-glutamate[20] at a concentration C_0 = 10 mM on a glass slide. Encapsulate the droplet by covering it with a circular PDMS chamber (diameter d = 5 mm, height h = 250 µm).
2. Place the glass slide on a microscope stage and expose the entire chamber for 20 ms to an LED beam at a wavelength of 395 nm (power 295 mW) by using a 4x objective (numerical aperture [NA] = 0.13).
3. Open the PDMS chamber and extract a droplet (1 µL) for analysis with a UV-Vis spectrophotometer.
4. Repeat steps 4.1−4.3 for different durations of LED illumination of 0.1 s, 0.5 s, 2.5 s, 25 s, 250 s (or until saturation of the chemical reaction) and 0 s (to obtain the background). Replicate the procedure steps 4.1−4.4 at least 3x (here, 4x).
5. From the absorption spectrum, extract the value at 405 nm, which represent the peak in the absorption spectrum of the cage molecule[21]. To determine the rate k of the chemical uncaging reaction by the LED exposure[14], use the following first-order kinetics equation for the numerical fit of the experimental data[17]

$$C(t) = C_0 (1 - e^{-kt}), \quad \text{(Eq. 1)}$$

where $C(t)$ is the value of the absorption spectrum of the solution at 405 nm (after background removal) with an uncaging time of t seconds. For small uncaging time t such that kt 1, Eq. 1 can be simplified to the linear formulation

$$C(t) = C_0 kt. \quad \text{(Eq. 2)}$$

5. Single Chemical-pulse Experiment

1. Maintain the microfluidic channel under vacuum for 20 min to reduce the gas concentration within the PDMS so that bubbles are less likely to form during the filling process.
2. Extract the channel from the vacuum pump and immediately introduce the dilute bacterial suspension in 1 mM MNI-caged-*L*-glutamate in artificial seawater into the microchannel gently using a micropipette to avoid flagellar damage by mechanical shearing forces (here, the entire filling process took 5-10 s). After filling the channel with the bacterial suspension, suck the solution in excess with paper towel, and seal inlet and outlet with PDMS plugs by gently pressing them into the holes.
   NOTE: In this way, fluid flow in the chamber is prevented.
3. Place the microchannel onto a microscope stage and move the stage to set the field of view in mid-channel. Set up the microscope to perform imaging in phase contrast (4x objective) at a frame rate of 12 fps.
   NOTE: This value can be varied but should not be less than 10 fps to allow reconstruction of the bacterial trajectories through image analysis (see protocol section 7).
4. Set the pinhole of the LED beam at the minimum aperture. By setting the exposure time of the camera to 5 s, record a few frames to obtain precise measurements of the spatial location and size of the LED beam.
   NOTE: The LED light source connects to the microscope's epi-fluorescence illuminator via liquid light guide connection. The LED beam does not affect video capturing, because video acquisition and LED stimulation are commanded independently via software.
5. Perform continuous imaging for a total duration of 10 min (20 min for the largest chemical pulse), and simultaneously activate the focused LED beam at 395 nm for the desired duration (in this experiment, t = 20 ms, 100 ms, 500 ms) at a user-defined time point (here, 10 s after the start of the video acquisition) via microscope software. To obtain multiple replicates of the same process, move the stage to record the bacterial response over different positions of the microfluidic channel. Replicate this procedure for each pulse size, using a new microchannel.
   NOTE: The uncaging process generates an axisymmetric cylindrical pulse that diffuses radially outwards in the imaging plane.
6. Conduct separate experiments without chemical uncaging at higher magnification (20x objective, NA = 0.45) at a higher frame rate (50 fps) to record the unbiased swimming motion of the bacteria.

6. Multiple Chemical-pulse Experiment

1. Maintain the millifluidic chamber under vacuum for 20 min.
2. Place the Petri dish containing the millifluidic chamber onto a microscope stage. Fill the chamber below the membrane with the dilute bacterial suspension (here, the entire filling process took 10−15 s) of GFP-fluorescent *V. ordalii* in 1 mM MNI-caged-*L*-glutamate solution in artificial seawater. After filling the channel with the bacterial suspension, suck the solution in excess with paper towel, and seal inlet and outlet with PDMS plugs by gently pressing them into the holes.
   NOTE: In this way, fluid flow in the chamber is prevented. To allow better visualization of bacteria in this setup where the imaging occurs through the nanoporous membrane, it is strongly recommended to use fluorescent strains instead of the wild type (as used in the single chemical-pulse experiment).
3. Fill a syringe with an artificial seawater solution of 1 mM MNI-caged-*L*-glutamate and attach tubing to the inlet and outlet of the washing channel above the membrane.
4. Connect the tubing to a waste reservoir and ensure that the tubing is entirely submerged in the fluid waste reservoir to avoid pressure oscillations.
5. Set the appropriate flow rate on the syringe pump (here, 50 µL min^{-1}) to obtain the desired mean flow rate in the washing channel, which depends on the channel geometry.
6. Start the syringe pump to establish the flow in the washing channel above the membrane.
7. Run the software controlling the LED beam and microscope stage to generate user-defined sequences of pulses at different locations and with different intensities.
   NOTE: The continuous flow of the artificial seawater solution of 1 mM MNI-caged-*L*-glutamate in the washing channel above the membrane replenishes the caged compound solution and washes the spent medium from the bacterial arena.
8. Record video using a 4x objective at regular time intervals over a period of several hours and over multiple contiguous locations to cover a large surface (here, 1 cm x 1 cm, **Figure 1F**).

7. Image Analysis and Data Analysis

1. Reconstruction of the bacterial trajectories
   1. From the movies recorded with the 4x objective, reconstruct the bacterial trajectories using tracking software[17].
      NOTE: These trajectories represent the 2D projections of the 3D bacterial motion in the microchannel.
   2. From the reconstructed bacterial trajectories, determine the radial drift velocity of each swimming individual by projecting its swimming speed over the direction towards the center of the chemical pulse (**Figure 2D**). For the visualization of the spatio-temporal dynamics of the radial drift velocity, use a binning grid with spatial size 75 µm x 75 µm and temporal window of 5−10 s interval (**Figure 2D,E**).
      NOTE: Because of the cylindrical symmetry of the process, data can be analyzed in polar coordinates and averaged over the angular dimension (**Figure 3**).
   3. From the reconstructed bacterial trajectories, determine the spatio-temporal dynamics of the distribution of bacteria as they respond to the chemical pulses (**Figure 2E**).

4. From the higher resolution movies recorded with the 20x objective during the single-pulse experiments, extract the distribution of swimming speed and run time for the bacterial population as they respond to the chemical pulse (**Figure 4**).

2. Estimate the diffusion coefficient of bacteria by considering the dissipation dynamics of the bacterial population after chemotaxis is completed[17] (here, for $t > 300$ s; **Figure 3**).
3. Estimate the diffusion coefficient of glutamate by applying the Stokes-Einstein equation

$$D_C = k_B T/(6\pi\eta r_G), \quad \text{(Eq. 3)}$$

where the amino acid molecules are assumed to be spherical particles with hydrodynamic radius[22] r_G, k_B is the Boltzmann constant (1.38 x 10^{-23} m^2 kg s^{-2} K^{-1}), T is the temperature (296 K), and η is the dynamic viscosity of the artificial seawater (salinity 36 g kg^{-1}) at 23 °C (10^{-3} Pa s)[23]

Representative Results

We used the microfluidic and millifluidic devices (**Figure 1**) to study bacterial accumulation profiles under dynamic nutrient conditions. Bacterial trajectories were extracted from recorded videos acquired by phase contrast microscopy of the accumulation-dissipation dynamics of a bacterial population following a chemical pulse released by photolysis (**Figure 2** and **Figure 3**). By averaging millions of trajectories, the spatiotemporal dynamics of the radial drift velocity and bacterial concentration were obtained. Statistics describing the swimming in the absence of a chemical gradient were obtained in separate experiments with higher spatial and temporal resolution (**Figure 4**).

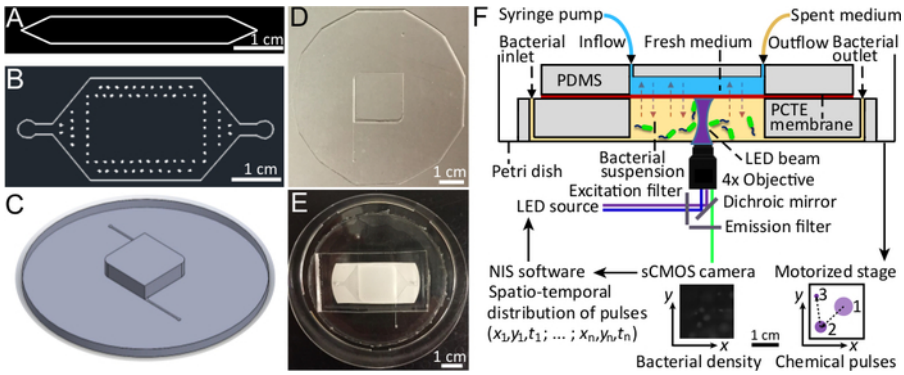

Figure 1: Microfluidic and millifluidic devices for bacterial experiments under dynamic nutrient conditions. (**A**) Photomask of the microfluidic channel used to observe the bacterial accumulation to a single chemical pulse. (**B**) Photomask of the microfluidics channel used to wash the millifluidic bacterial chamber for the multi pulse experiments. The small dots are micropillars (200 µm in size) that help the bonding of the membrane to the PDMS, and at the same time help prevent the membrane from buckling or collapsing in the center. (**C**) Design of the 3D printed master used to create the bacterial chamber. (**D**) The PDMS layer with the patterning of the bacterial chamber. (**E**) The complete millifluidic device (top view, PCTE membrane in white). (**F**) Schematic of the millifluidic device for the generation of dynamic nutrient conditions (side view). Optics ray diagram is shown on the bottom of the device, where a violet beam (395 nm) performs the uncaging of the chemoattractant, whereas an (independent) blue beam (470 nm) is used for the observation of fluorescent bacteria (harboring pGFP) through a sCMOS camera, which captures the bacterial density (bottom centre). The device is placed on a motorized stage (bottom right), which can be moved in the x-y plane to release chemical pulses at user-defined positions (controlled via NIS software, bottom left). Please click here to view a larger version of this figure.

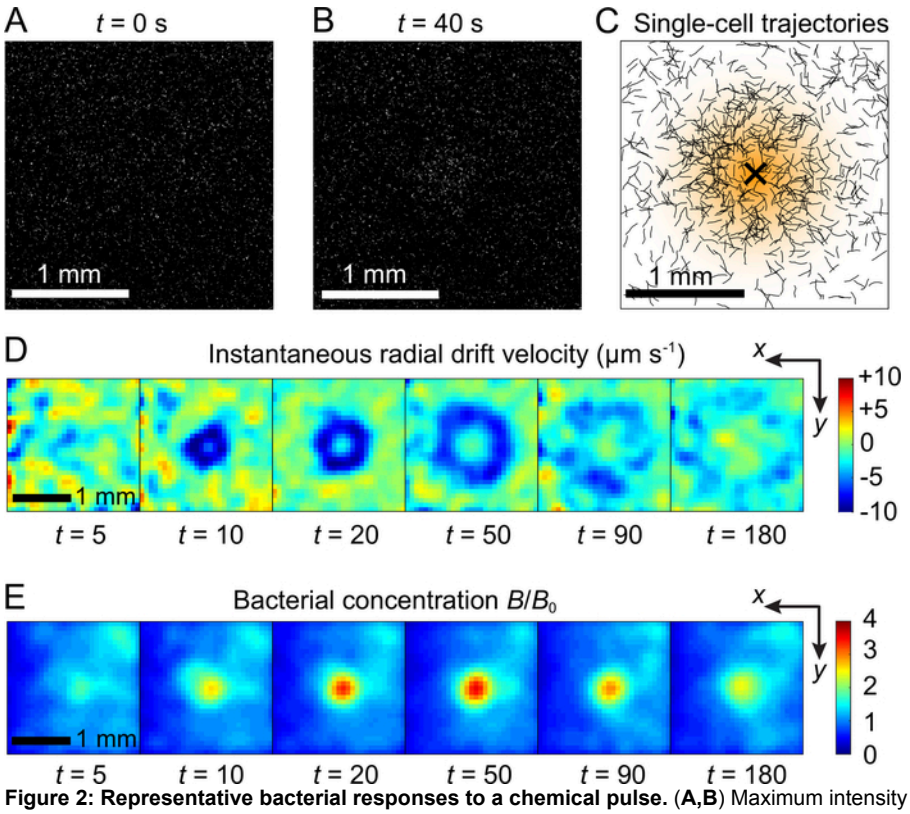

Figure 2: Representative bacterial responses to a chemical pulse. (**A,B**) Maximum intensity projection showing bacterial position (white) over a 0.5 s interval, shown (**A**) immediately following, and (**B**) 40 s after the pulse release (objective: 4x, NA = 0.13, Ph 2; video recording at 12 fps). (**C**) Bacterial trajectories (black) shown 60 s after the pulse release. The shaded region represents the chemical pulse released by photolysis at t = 0 s in the middle of the field of view (black cross), which subsequently diffuses. Trajectories were reconstructed using custom in-house software. (**D,E**) Temporal dynamics of the radial drift velocity (**D**) and of the bacterial concentration (**E**) following a pulse release in the center of the field of view. In panel D, negative values of the drift velocity (in blue color) correspond to directed chemotactic motion towards the center of the pulse. This figure has been modified after Brumley et al.[17]. Please click here to view a larger version of this figure.

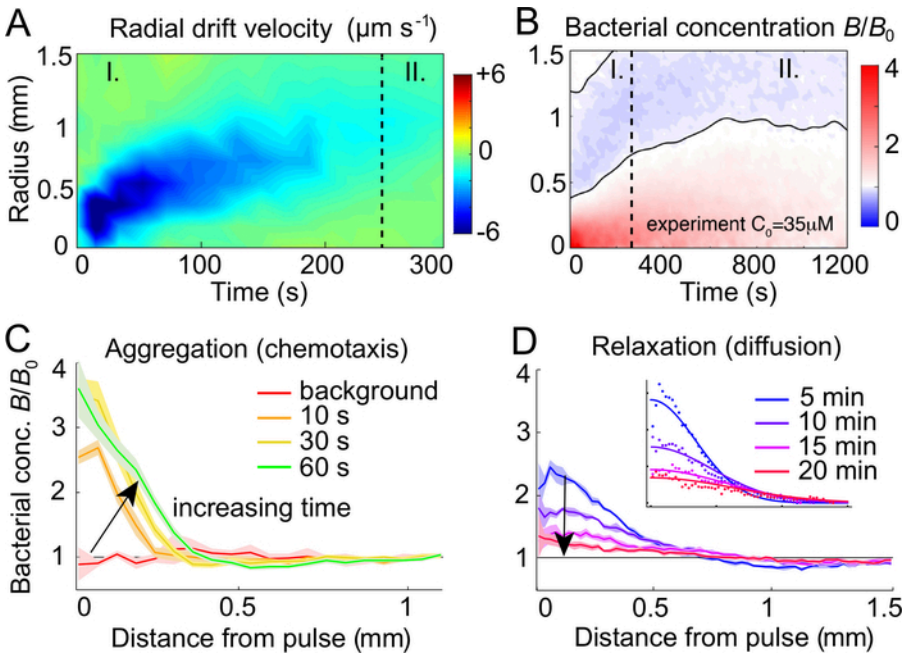

Figure 3: Spatio-temporal profiles of the radial drift velocity and bacterial concentration following a chemical pulse release. (**A**,**B**) The radial drift velocity (**A**) and the bacterial concentration (**B**) as a function of time and distance from the center of a 35 μM glutamate pulse. In panel A, negative values of the drift velocity (in blue color) correspond to directed chemotactic motion towards the center of the pulse. Values were calculated by averaging over all trajectories. The black dashed line at t = 250 s roughly delimits the period of active chemotaxis (blue shading in panel A, region I), after which the cells diffuse isotropically outward (green shading in panel A, region II). (**C**) Bacterial concentration (rescaled over the background B_0) as a function of distance at t = 10, 30, 60 s after the creation of a diffusing chemical pulse. Bacteria aggregate close to the site of the pulse due to chemotaxis. (**D**) Bacterial concentration takes ~20 min to relax to the background B_0 by bacterial diffusion. The inset shows the fit of the diffusive spreading with a diffusion coefficient of D_B = 165 μm^2 s^{-1}. Panels A, C, and D have been modified from Brumley et al.[17]. Please click here to view a larger version of this figure.

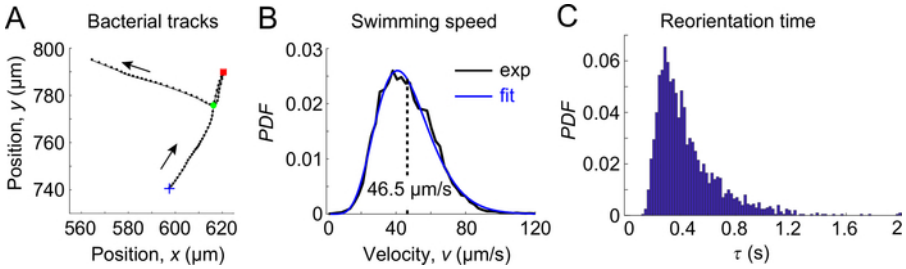

Figure 4: Swimming statistics for a bacterial population in the absence of chemical gradients. (**A**) Trajectories represent the two-dimensional projections of the three-dimensional bacterial motion in the microchannel. Bacterial trajectories are extracted using a custom in-house tracking script. Here the blue cross indicates the start of the track, and red and green symbols indicate reorientation events. Data were recorded at 50 fps with a 20x objective, NA 0.45. (**B**) Probability distribution of measured bacterial swimming speed (black) together with a gamma distribution fit (blue). Because the depth of focus when imaging with a 20x objective (NA 0.45) is only a few microns[24], the recorded trajectories are essentially planar and measurements of the swimming speed are not biased by the projection. (**C**) Probability distribution of the time between successive reorientations. These data were required to effectively calibrate an individual based model that takes into account the reorientation pattern, the distribution of swimming speed, and the reorientation statistics of the organisms. This figure has been modified from Brumley et al.[17]. Please click here to view a larger version of this figure.

Discussion

This method allows researchers to study bacterial chemotaxis under controlled, dynamic gradients in micro- and millifluidic devices, enabling reproducible data acquisition. The near-instantaneous creation of chemical pulses at the microscale by photolysis aims to reproduce the types of nutrient pulses that bacteria encounter in the wild from a range of sources, for example, the diffusive spreading of plumes behind sinking marine particles[25], or the nutrient spreading from lysed phytoplankton cells[26].

We presented two applications of this method: 1) the release of a single chemical pulse to study the bacterial accumulation−dissipation dynamics starting from uniform conditions, and 2) the release of multiple pulses to characterize the bacterial accumulation profiles under non-equilibrium nutrient conditions. The first application is particularly suited to characterize the behavioral responses of microbes when first encountering a nutrient source. Under such conditions, in which the concentration of chemoattractant molecules is extremely low, the early phase of chemotaxis is dominated by the stochastic binding−unbinding events of chemoattractant molecules to the chemoreceptors[17]. Our method, by rapidly and precisely releasing a known mass of chemoattractant in a zero-nutrient background, offers significant advantages over previous approaches to

characterize the bacterial response under dynamic conditions[27,28,29]. Advantages include knowing the full distribution of chemoattractant at all locations and at all times (since its diffusivity is known), and completely avoiding the generation of fluid flow that is inherently associated with other devices, such as the microinjector[27] or three-inlet geometries[30].

In the second application, the chemical pulses occur in a large, quasi-2D domain according to a user-defined sequence in space and time that is fully customizable via software, which can be used to impose random sequences or particular patterns. Importantly, this method provides a powerful link between the high-resolution behavioral dynamics of bacterial chemotaxis and nutrient uptake over timescales of seconds and long-term dynamics, such as growth and potentially evolution. The bacterial arena is considerably larger (2 cm x 2 cm) than the spatial range of chemical interaction of the bacteria with a single pulse (from hundreds of micrometers for the smallest pulses to a few millimeters for the largest pulses). Key to the maintenance of a low chemical background (much lower than the concentration of the chemical pulses at their release) is the inclusion of the nanoporous PCTE membrane sandwiched between the two PDMS layers[18]. By applying a fluid flow in the microfluidic channel placed at the top of the device, a continuous wash-out of the uncaged compounds and spent medium in the bacterial arena is realized by means of molecular diffusion through the nanoporous membrane, without creating flow in the test section of the device where bacteria are located (**Figure 1**).

By modulating the focused LED beam in time, amplitude, size, and geometry, photorelease technology endows the experimenter with great flexibility to generate different types of chemical environments. At the same time, while the tests presented here were performed under quiescent conditions, our method can be further expanded to test bacterial chemotaxis under different flow configurations. By faithfully reconstructing the bacterial accumulation dynamics through video microscopy, our method generates large quantities of high quality data that can be used to estimate the statistics of bacterial behavior and the potential nutrient uptake by bacterial cells. Our experimental microfluidic approach, mimicking nutrient landscapes that bacteria might face under natural environmental conditions, allows the systematic study of the foraging behavior of microbial species that are essential in the cycling of nutrients at the macroscopic scale[2,3]. As such, the type of data generated through this methodology is useful to effectively calibrate population uptake rates and better derive nutrient kinetics in mesoscale ecosystem models.

The fabrication of the PDMS molds to make the large bacterial arena was performed using a commercial 3D printing service. However, similar results can be achieved using a high-end 3D printer in house, with a resolution of 50−100 µm required to resolve the smallest features of the microchannel designs. A smooth surface of the 3D-printed material for the PDMS mold is required to achieve a good bonding between the cast PDMS and the other surfaces of the device (i.e., glass, polystyrene, PDMS). For our application, the use of a polystyrene Petri dish (90 mm x 15 mm) as the lower surface of the 3D arena presents two advantages over the use of a glass slide as commonly employed in microfluidics studies: first, it considerably reduces the attachment of bacterial cells compared to a glass surface (although attachment might depend on the particular surface properties of the microbe under consideration); second, it provides secondary containment, which can prevent leakage of media over microscopy equipment in the case of spills. The PDMS mold curing process typically occurs at a high temperature (70−80 °C), but in this application the experimenter must bake the PDMS mold at a considerably lower temperature (45 °C in the current case, see **Table of Materials**), below the heat deflection and the melting temperature of the material used for the 3D printing of the master. The lower baking temperature considerably lengthens the curing process (overnight), but does not change the mechanical and chemical properties of the PDMS.

Although our method has been applied to one particular combination of bacteria and chemoattractant, the methodology is suitable to test diverse biological processes, including nutrient uptake or antibiotic exposure, and can be applied to model systems of different species and chemoattractants, given that a myriad of molecules have been (or can be) caged[8]. One potential limitation arises from the costs of commercially available caged compounds, but these costs are comparable to those incurred when using the molecular probes typically employed in the life sciences for cell viability, counting, or intracellular staining. Notwithstanding this potential limitation, the proposed methodology may find broad applications across biophysical and biomedical sciences, to characterize early responses and adaptation dynamics of microbial populations at single cell resolution to dynamic chemical gradients.

Disclosures

The authors have nothing to disclose.

Acknowledgments

The authors thank the FIRST microfabrication facility at ETH Zurich. This work was supported by an Australian Research Council Discovery Early Career Researcher Award DE180100911 (to D.R.B.), a Gordon and Betty Moore Marine Microbial Initiative Investigator Award GBMF3783 (to R.S.), and a Swiss National Science Foundation grant 1-002745-000 (to R.S.).

References

1. Armitage, J.P., Lackie, J.M. *The biology of the chemotactic response.* Cambridge University Press. (1991).
2. Azam, F., Malfatti, F. Microbial structuring of marine ecosystems. *Nature Reviews Microbiology.* **5** (10), 782-791 (2007).
3. Buchan, A., LeCleir, G.R., Gulvik, C.A., González, J.M. Master recyclers: features and functions of bacteria associated with phytoplankton blooms. *Nature Reviews Microbiology.* **12** (10), 686-698 (2014).
4. Whitesides, G.M., Ostuni, E., Takayama, S., Jiang, X., Ingber, D.E. Soft lithography in biology and biochemistry. *Annual Review of Biomedical Engineering.* **3**, 335-373 (2001).
5. Segall, J.E., Block, S.M., Berg, H.C. Temporal comparisons in bacterial chemotaxis. *Proceedings of the National Academy of Sciences of the United States of America.* **83** (23), 8987-8991 (1986).
6. Waite, A.J. et al. Non-genetic diversity modulates population performance. *Molecular Systems Biology.* **12** (12), 895 (2016).
7. Stocker, R. Marine Microbes See a sea of gradients. *Science.* **338** (6107), 628-633 (2012).
8. Ellis-Davies, G.C.R. Caged compounds: photorelease technology for control of cellular chemistry and physiology. *Nature Methods.* **4** (8), 619-628 (2007).

9. Kaplan, J.H., Somlyo, A.P. Flash photolysis of caged compounds: New tools for cellular physiology. *Trends in Neurosciences.* **12** (2), 54-59 (1989).
10. Ando, H., Furuta, T., Tsien, R.Y., Okamoto, H. Photo-mediated gene activation using caged RNA/DNA in zebrafish embryos. *Nature Genetics.* **28** (4), 317-325 (2001).
11. England, P.M., Lester, H.A., Davidson, N., Dougherty, D.A. Site-specific, photochemical proteolysis applied to ion channels in vivo. *Proceedings of the National Academy of Sciences of the United States of America.* **94** (20), 11025-11030 (1997).
12. Fino, E. RuBi-Glutamate: Two-photon and visible-light photoactivation of neurons and dendritic spines. *Frontiers in Neural Circuits.* **3**, (2009).
13. Khan, S., Spudich, J.L., McCray, J.A., Trentham, D.R. Chemotactic signal integration in bacteria. *Proceedings of the National Academy of Sciences of the United States of America.* **92** (21), 9757-9761 (1995).
14. Sagawa, T. et al. Single-Cell E. coli Response to an Instantaneously Applied Chemotactic Signal. *Biophysical Journal.* **107** (3), 730-739 (2014).
15. Xie, L., Lu, C., Wu, X.L. Marine Bacterial Chemoresponse to a Stepwise Chemoattractant Stimulus. *Biophysical Journal.* **108** (3), 766-774 (2015).
16. Jikeli, J.F. et al. Sperm navigation along helical paths in 3D chemoattractant landscapes. *Nature Communications.* **6**, 7985 (2015).
17. Brumley, D.R. et al. Bacteria push the limits of chemotactic precision to navigate dynamic chemical gradients. *Proceedings of the National Academy of Sciences of the United States of America.* **116** (22), 10792-10797 (2019).
18. Aran, K., Sasso, L.A., Kamdar, N., Zahn, J.D. Irreversible, direct bonding of nanoporous polymer membranes to PDMS or glass microdevices. *Lab on a Chip.* **10** (5), 548 (2010).
19. ZoBell, C.E. The cultural requirements of heterotrophic aerobes. *Journal of Marine Research.* **4**, 42-75 (1941).
20. Canepari, M., Nelson, L., Papageorgiou, G., Corrie, J.E.T., Ogden, D. Photochemical and pharmacological evaluation of 7-nitroindolinyl-and 4-methoxy-7-nitroindolinyl-amino acids as novel, fast caged neurotransmitters. *Journal of Neuroscience Methods.* **112** (1), 29-42 (2001).
21. Trigo, F.F., Corrie, J.E.T., Ogden, D. Laser photolysis of caged compounds at 405nm: Photochemical advantages, localisation, phototoxicity and methods for calibration. *Journal of Neuroscience Methods.* **180** (1), 9-21 (2009).
22. Ribeiro, A.C.F. et al. Mutual diffusion coefficients of L-glutamic acid and monosodium L-glutamate in aqueous solutions at T=298.15K. *The Journal of Chemical Thermodynamics.* **74**, 133-137 (2014).
23. Sharqawy, M.H., Lienhard, J.H., Zubair, S.M. Thermophysical properties of seawater: a review of existing correlations and data. *Desalination and Water Treatment.* **16** (1−3), 354-380 (2010).
24. *Nikon depth of field calculator.* https://www.microscopyu.com/tutorials/depthoffield. (2019).
25. Kiørboe, T., Thygesen, U.H. Fluid motion and solute distribution around sinking aggregates: II. Implications for remote detection by colonizing zooplankters. *Marine Ecology Progress Series.* **211**, 15-25 (2001).
26. Blackburn, N., Fenchel, T., Mitchell, J. Microscale nutrient patches in planktonic habitats shown by chemotactic bacteria. *Science.* **282** (5397), 2254-2256 (1998).
27. Stocker, R., Seymour, J.R., Samadani, A., Hunt, D.E., Polz, M.F. Rapid chemotactic response enables marine bacteria to exploit ephemeral microscale nutrient patches. *Proceedings of the National Academy of Sciences of the United States of America.* **105** (11), 4209-4214 (2008).
28. Altindal, T., Chattopadhyay, S., Wu, X.L. Bacterial chemotaxis in an optical trap. *PLoS ONE.* **6** (4), e18231 (2011).
29. Zhu, X. et al. Frequency-Dependent *Escherichia coli* Chemotaxis behavior. *Physical Review Letters.* **108** (12), (2012).
30. Baraban, L., Harazim, S.M., Sanchez, S., Schmidt, O.G. Chemotactic behavior of catalytic motors in microfluidic channels. *Angewandte Chemie International Edition.* **52** (21), 5552-5556 (2013).

